Masyukov, Maxim; Vainshtein, Sergey; Mallat, Juha; Taylor, Zachary

Contactless Terahertz Sensing of Ultrafast Switching in Marx Generator Based on Avalanche Transistors

Published in:
IEEE Electron Device Letters

DOI:
10.1109/LED.2022.3199996

Published: 01/10/2022

Document Version
Peer-reviewed accepted author manuscript, also known as Final accepted manuscript or Post-print

Please cite the original version:
Masyukov, M., Vainshtein, S., Mallat, J., & Taylor, Z. (2022). Contactless Terahertz Sensing of Ultrafast Switching in Marx Generator Based on Avalanche Transistors. *IEEE Electron Device Letters*, *43*(10), 1724-1727. Article 9861612. https://doi.org/10.1109/LED.2022.3199996

Contactless Terahertz Sensing of Ultrafast Switching in Marx Generator Based on Avalanche Transistors

Maxim Masyukov, *Student Member, IEEE,* Sergey Vainshtein, Juha Mallat, and Zachary Taylor, *Member, IEEE*

***Abstract*—In this paper, we have studied the temporal evolution of switching for each stage of the Marx generator with picosecond temporal and millimeter spatial resolutions employing terahertz measurements. The Marx circuit utilizes collapsing-field-domain (CFD)-based avalanche switches, which are formed in a bipolar GaAs structure and result in the picosecond speed of powerful carrier generation and electrical switching. The application of the CFD-based avalanche switches emitting mm-wave pulsed radiation in the Marx generator provides a unique opportunity to accurately track the switching instants for each of the circuit stages with a picosecond time precision. The collapsing domains cause the sub-THz pulses radiated by each of the avalanche switches, and the same domains generate the electron-hole plasma thus causing simultaneously the electrical switching. In this work, we report the direct measurements of the switching instants for each of the four stages Marx generator and suggest an interpretation of non-trivial experimental results.**

***Index Terms*—Marx generators, avalanche breakdown, solid-state terahertz (THz) pulsed source.**

I. Introduction

Marx circuits are typically used to generate high-voltage pulses [1], but can also be used to significantly increase the peak current across a load [2] and include a broad variety of applications [3]–[5]. They utilize solid-state switches [6] where the switching mechanism is triggered by a voltage, exceeding the threshold, applied between the anode and cathode, or, alternatively, by the dV/dt effect, when the turn-on is initiated by a sharp voltage ramp. The same physics also works in avalanche transistors [2].

One hypothesis regarding the operation of the Marx generator is that switching happens simultaneously in all stages. However, this claim is difficult to experimentally verify, at least for high-speed ns- and sub-ns switching times, since high-speed oscilloscope probing of individual switching events is complicated by spatially and temporally varying potentials on the ground plane. Alternatively, free space microwave pulsed emission can be used for the switching instants detection but it is very challenging to attribute the pulses to a particular transistor: the characteristic wavelengths of emitted ultrawideband microwave pulses ($\approx$ few dm) typically exceed the size of the entire circuit board, further confounding source localization.

This work was supported in part by Jane and Aatos Erkko Foundation.

The authors are with the MilliLab, Department of Electronics and Nanoengineering, Aalto University, P.O. Box 15500, 00076 Aalto, Finland. Corresponding author: Maxim S. Masyukov (e-mail: maxim.masyukov@aalto.fi).

Dr. Sergey N. Vainshtein is also with the CAS group, Faculty of Information Technology and Electrical Engineering, the University of Oulu, FIN-90014 Oulu, Finland

Manuscript received XX.XX.XXXX; revised XX.XX.XXXX.

Terahertz sensing can shed additional light on this problem. Ultra-high amplitude, ultra-narrow collapsing field domains (CFDs) in the collector of a GaAs avalanche transistor [7], are caused by negative differential mobility at extreme fields [8] and lead to ultrafast electrical switching [9] due to powerful ionization. Concomitant sub-THz current oscillations across the conductive channels [10] result in electromagnetic waves emission when the current is coupled to an on-chip antenna. These features enable embedding ultrafast picosecond-range GaAs avalanche transistors in a Marx-bank high-voltage pulse generator circuit [11] and analyzing the sub-THz pulses radiated by each transistor.

In this letter, we investigate a four-stage CFD-based Marx generator and demonstrate a contactless sensing method for ultrafast switching analysis in each stage by means of quasioptical terahertz direct detection. CFDs associated with the avalanche switching produce millimeter-wave emissions corresponding to 200 GHz. The free space wavelengths are similar in size to the antenna coupled to the avalanching transistor, and consequently, the switching instants of different transistors can be easily separated by spatially isolating each emission. Since CFD-based switches can be incorporated into other solid-state devices and circuits, the methodology may have applications in modern optoelectronics metrology and allow fully contactless and nondestructive sensing and characterization of switching in avalanche semiconductor devices by quasioptic means.

II. Experimental setup and device under test

Fig. 1 shows a diagram of a pulsed 200 GHz source consisting of mm-size on-chip bow-tie antenna (A_i) (a) and CFD-avalanching, GaAs transistor (b) [7]. The equivalent circuit of the Marx generator and its printed circuit board (PCB) view are shown in Fig. 1 (c) and (d), respectively. The on-chip antenna can be approximated as an RLC-circuit shown in the insert (e) of the same figure with the following parameters: $C_a = 85\ fF$, $L_a = 8\ pH$ and $R_a = 35\ \Omega$. This low-inductance (L_a) antenna circuit interacts with CFDs in the avalanche switch thus affecting sub-THz oscillations and the emission, but does not affect the avalanche switching itself due to the small C_a. Capacitors (C) and inductors (L) form the circuit loop which operates in a sub-ns avalanche switching regime ($1-10\ GHz$ band), while $200\ GHz$ oscillations caused by CFDs cannot penetrate this large inductance ($L_{total} > 4 \cdot L$) circuit. Unlike the devices with base-triggering described in Ref. [7], the avalanche switching in the current device is initiated by the avalanche breakdown of the base-collector junction at $V_b \approx 22\ V$.

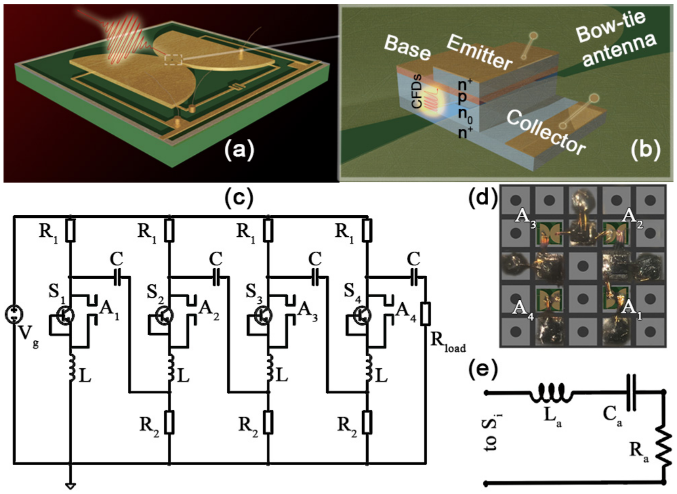

Fig. 1. (a) The on-chip realization of the CFD-based switch (1×1 mm in size); (b) the CFD switch and its connection with a bow-tie antenna; (c) the circuit diagram of the solid-state Marx generator: $R_1 = 260\ k\Omega$, $R_2 = 7\ k\Omega$, $C = 2.7\ pF$, $L = 1.5\ nH$, $R_{load} = 10\ \Omega$; (d) an artistic image of the Marx circuit PCB topology; (e) the equivalent circuit of the on-chip antenna A_i: $C_a = 85\ fF$, $L_a = 8\ pH$ and $R_a = 35\ \Omega$.

The topside of the PCB with the device (Fig. 1 (d)) is orientated towards the elliptic mirror shown in Fig. 2, thus the Marx generator (MG) is located in the first focal point of the mirror. An X-Y-Z translation stage allows the switches S_{1-4} to be positioned in the first focus of the elliptic mirror individually. A zero bias Schottky diode detector (170-260 GHz band, VDI WR4.3ZBD with a WR-5.1 conical horn) is placed at the second focus of the mirror and records sub-THz pulses emitted by each of the switches. The signal from the Schottky detector is then amplified ($0.1 - 26\ GHz$ / $30\ dB$ MITEQ Microwave Amplifier) and delivered to the oscilloscope (Femtoscope, Eltesta), which is triggered by the pulse across the load resistor ($R_{load} = 10\ \Omega$) recorded at the second input. We have selected an optimized R_{load} which is about equal to the output impedance of the entire circuit, provides relatively high current amplitude, and gives as narrow the current pulse as possible but prevents, however, an appearance of relaxation oscillations. The more detailed studies of impedance matching in more complicated Marx generators and their characteristics are provided in Ref. [3], [12], [13]. The biasing voltage of $V_g = 23\ V$ is sufficient for periodic self-triggering of the Marx circuit without an external generator with a repetition rate of $1.5 - 2\ MHz$ determined by the bias voltage and $(R_1 + R_2) \times C$ product.

III. Results and Discussion

Transistor S_1 (Fig. 1) has a breakdown voltage $V_{b_{S_1}} \approx 21.9\ V$, while others $V_{b_{S_{2-S_4}}} \approx 22$ V. Initial charging of the capacitor C in the first stage within $t \approx 0.5\ \mu s$ increases the voltage across S_1 to the breakdown value, leading to switching of S_1, and then a negative voltage ramp is applied to the emitter of S_2, triggers its switching defined by mechanisms discussed above. Then, even higher voltage ramps trigger emitters S_3 and S_4. Switching of all four stages results in a series connection of all capacitors C, and the voltage

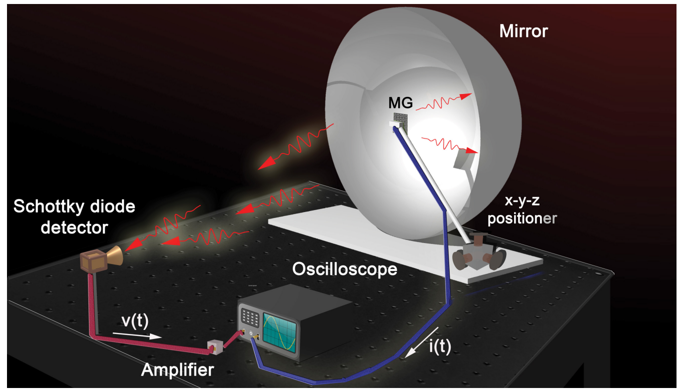

Fig. 2. A schematic representation of the experimental setup.

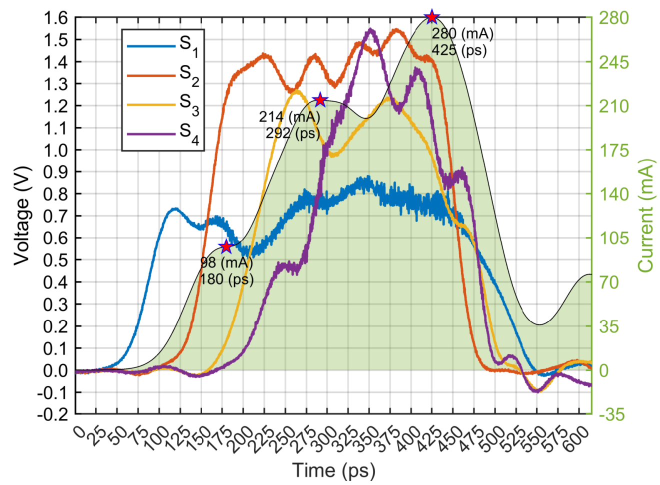

Fig. 3. The current detected at R_{load} and emission from the CFD structures measured by the Schottky detector with 30 dB amplifier. The peak values of current ($\star$) are highlighted.

$\sum_{i=1}^{4} V_{S_i}$ minus residual voltages across S_{1-4} is detected at the load resistor R_{load}. The current pulse across the load is shown in Fig. 3, after numerical reduction of parasitic inductance [7].

The oscillatory behavior of the current pulse rising edge in Fig. 3 is associated with corresponding instants of the transistors S_{1-4} switching. We attribute the peak in the rising sub-THz pulse intensity emitted by a particular transistor to the moment when the ionization in CFDs results in a significant increase of electron-hole plasma density in the conductive channel, and the voltage across the transistor starts reducing due to the CFDs shrinkage [9], [14]. Then the voltage across other transistors and the load grows, resulting in the rise of the current. For example, the ionization peak in transistor S_1 can be attributed to the instant at $t = 120\ ps$ (with a voltage at the Schottky detector $V_{d_1}(120\ ps) = 0.73\ V$), and the corresponding increase in the current limited by the inductance lasts till $t = 180\ ps$. Further boost of the current between $200\ ps$ and $292\ ps$ is related to the combined effect of S_2 and S_3 switching, whereas the final current rise between $350\ ps$ and $425\ ps$ is caused by the switching of transistor S_4. The significant delays in switching processes between the stages,

This article has been accepted for publication in IEEE Electron Device Letters. This is the author's version which has not been fully edited and
content may change prior to final publication. Citation information: DOI 10.1109/LED.2022.3199996

ranging between 60 ps and 70 ps, are comparable with the switching time of each transistor. Finally, we attribute the abrupt break in radiation from switches S_{2-4} at $t = 500$ ps (Fig. 3) to the domains collapse at an extremely high carrier density [8], [9], [14]. Well pronounced differences in the amplitude of the radiation from S_1 and other transistors (S_{2-4}) are enumerated below.

The interpretation of inter-cascade switching delays relies on the earlier findings [9], [10], [14] related to the CFD phenomenon. The first avalanche switching phase caused by the electron injection from the emitter and hole avalanche injection from the subcollector occurs when the current density exceeds the critical value of 30 kA/cm^2 (for the transistors with the collector doping of 2×10^{16} cm^{-2} used here), and the entire emitter-base perimeter participates in the switching (with the conducting area of ≈ 10 μm^2). Thus, a relatively slow (up to 1 ns) transient of the first switching phase occurs when the current across the transistor exceeds 3 mA.

The second, ultrafast switching phase, accompanied by the CFD formation and filamentation, starts when the current density exceeds ≈ 300 kA/cm^2 across the filament with an area of 2 μm^2, which requires the total current of at least 6 mA across the transistor. When $V_{b_{S_1}}$ is reached, the resistance R_1 is large, and the current for the first avalanche switching phase is supplied only by the capacitors chain C, load resistor R_{load}, and switched-off (so far) transistors S_{2-4}. The displacement current across the barrier capacitances of S_{2-4} ($C_b \approx 1.5$ fF for each transistor and 0.5 fF for the series connection of three transistors S_{2-4}) provides a current of 3 mA across the switch S_1, which supports the first switching phase in S_1, but cannot provide the current level for the second switching phase.

The further switching scenario of the Marx circuit is as follows. "Slow" reduction in the voltage across S_1 within the first phase redistributes the voltage across the chain S_{1-4} which causes the avalanche process initiation in the switches S_2, S_3 and S_4. After the delay, slowly switching transistors S_{2-4} provide a current of more than 6 mA across S_1 sufficient for ultrafast filamentary switching. Fast reduction in the voltage across S_1 increases the voltage across the transistors S_{2-4} still further, and then transistor S_2 reaches the threshold of filamentary CFD-assisted switching. The same process is repeated then for S_3 and later for S_4.

Thus, we attribute the inter-stage switching delays to the time intervals required for the interphase changeover in each transistor. Namely, S_1 realizes CFD-based filamentary switching with a limited current supply across S_{2-4}, while S_2 starts the ultrafast switching when the voltage across S_3 and S_4 exceeds the breakdown level significantly, and the current supplied by S_2 is remarkably larger. The more it concerns the superfast switching process of S_3 and S_4. All in all, the ultrafast switching of S_1, which happens at the strongest external current limitation, should form the area of the switching filament as small as possible for the CFDs formation. This should result in domains with limited amplitude, and minimal conductivity in the channels during the entire current pulse. These features can explain the reduced radiation amplitude due to limited current oscillations in the antenna A_1, as demonstrated in Fig. 3. Furthermore, the radiation recorded from S_1 lasts longer than that from other transistors. We think that the electron-hole plasma density in the switching filament of the first transistor is lower (due to current limitation when the filament has been formed), and that is why the CFD collapse caused by access plasma density occurs in S_{2-4} earlier than in S_1.

Perfect switching synchronization of all stages utilizing ultrafast components likely requires a certain "smart" Marx circuit design, in which all the switches pass the first switching stage simultaneously and with identical conditions. In this case, the "voltage wave" running along the circuit stages would cause an ultrafast filamentary switching realized synchronously for all the transistors.

Additional verification of our findings has been performed with a similar circuit, in which triggering started not from S_1, but from S_4. The result is nearly identical, with similar interstage delays, but with the reverse switching order. Thus, the circuit can be implemented with an inverted switching process, but instead of negative voltage ramps applied to the emitters, it uses negative voltage ramps applied to collectors.

IV. Conclusion

In summary, a four-stage Marx generator circuit utilizing picosecond-range switches with simultaneous sub-THz emission has been investigated. Namely, a contactless method for terahertz sensing of ultrafast switching in Marx generator based on avalanche transistors has been proposed. A unique combination of picosecond temporal and millimeter spatial resolution has allowed the timing synchronization between the stages to be directly measured.

We have particularly observed that the current pulse generated by the Marx circuit can be approximately five times longer than the shortest sub-THz pulse ($\tau \approx 100$ ps) emitted by the last-switched transistor S_4. The significant increase in the current pulse duration across the load resistor is attributed to the following factors: the inter-stage switching delays, and the different duration of the domain regime in each transistor. The last one is affected by the time-dependent impedance of the entire circuit. Namely, transistor S_4 reaches its CFD switching mode when other transistors have already been switched. Thus, the circuit impedance does not strictly limit the current supplied by the external circuit, and the CFD carrier generation runs most efficiently that takes the shortest time. On the contrary, transistor S_1 switches at the highest impedance of the entire circuit, which reduces the efficiency of the CFD switching process, and the transient takes a longer time.

The discovered results suggest an idea for optimized temporal synchronization of picosecond components combined in the Marx circuit.

Acknowledgements

The authors also would like to thank Dr. V. Zemlyakov and Prof. I. Prudayev for fruitful discussions and comments. Prof. V. Mikhnev is acknowledged for providing the antenna parameters.

REFERENCES

[1] Z. Deng, Q. Yuan, S. Shen, J. Yan, Y. Wang, and W. Ding, "High voltage nanosecond pulse generator based on avalanche transistor Marx bank circuit and linear transformer driver," *Review of Scientific Instruments*, vol. 92, no. 3, p. 034715, March 2021, doi: 10.1063/5.0042523

[2] S. Vainshtein, J. Kostamovaara, R. Myllyla, A. Kilpela, and K. Maatta, "Automatic switching synchronisation of serial and parallel avalanche transistor connections," *Electronics Letters*, vol. 32, no. 11, pp. 950–952, June 1996, doi: 10.1049/el:19960660

[3] W. Stygar, K. LeChien, M. Mazarakis, M. Savage, B. Stoltzfus, K. Austin, E. Breden, M. Cuneo, B. Hutsel, S. Lewis *et al.*, "Impedance-matched Marx generators," *Physical Review Accelerators and Beams*, vol. 20, no. 4, p. 040402, Apr. 2017, doi: 10.1103/PhysRevAccelBeams.20.040402

[4] Y.-J. Chen, A. Neuber, J. Mankowski, J. Dickens, M. Kristiansen, and R. Gale, "Design and optimization of a compact, repetitive, high-power microwave system," *Review of Scientific Instruments*, vol. 76, no. 10, p. 104703, Oct. 2005, doi: 10.1063/1.2093768

[5] Z. Zhong, J. Rao, H. Liu, and L. Redondo, "Review on solid-state-based Marx generators," *IEEE Transactions on Plasma Science*, vol. 49, no. 11, pp. 3625–3643, Nov. 2021, doi: 10.1109/TPS.2021.3121683

[6] S. Shen, J. Yan, Y. Wang, G. Sun, and W. Ding, "Further investigations on a modified avalanche transistor-based Marx bank circuit," *IEEE Transactions on Instrumentation and Measurement*, vol. 69, no. 10, pp. 8506–8513, Oct. 2020, doi: 10.1109/TIM.2020.2993343

[7] S. N. Vainshtein, G. Duan, V. S. Yuferev, V. E. Zemlyakov, V. I. Egorkin, N. A. Kalyuzhnyy, N. A. Maleev, A. Y. Egorov, and J. T. Kostamovaara, "Collapsing-field-domain-based 200 GHz solid-state source," *Applied Physics Letters*, vol. 115, no. 12, p. 123501, Sept. 2019, doi: 10.1063/1.5091616

[8] S. Vainshtein, V. Yuferev, V. Palankovski, D.-S. Ong, and J. Kostamovaara, "Negative differential mobility in gaas at ultrahigh fields: Comparison between an experiment and simulations," *Applied Physics Letters*, vol. 92, no. 6, p. 062114, Feb. 2008, doi: 10.1063/1.2870096

[9] S. Vainshtein, V. Yuferev, and J. Kostamovaara, "Ultrahigh field multiple Gunn domains as the physical reason for superfast (picosecond range) switching of a bipolar GaAs transistor," *Journal of Applied Physics*, vol. 97, no. 2, p. 024502, Nov. 2005, doi: 10.1063/1.1839638

[10] S. N. Vainshtein, G. Duan, V. A. Mikhnev, V. E. Zemlyakov, V. I. Egorkin, N. A. Kalyuzhnyy, N. A. Maleev, J. Näpänkangas, R. B. Sequeiros, and J. T. Kostamovaara, "Interferometrically enhanced sub-terahertz picosecond imaging utilizing a miniature collapsing-field-domain source," *Applied Physics Letters*, vol. 112, no. 19, p. 191104, May 2018, doi: 10.1063/1.5022453

[11] Y. Gu, C. Zhang, W. Bian, S. Wu, and Z. Xu, "A novel modular pulse generator with high voltage gain and reduced number of capacitors," *IEEE Transactions on Plasma Science*, Feb. 2022, doi: 10.1109/TPS.2022.3140225

[12] T. Huiskamp and J. Van Oorschot, "Fast pulsed power generation with a solid-state impedance-matched Marx generator: Concept, design, and first implementation," *IEEE Transactions on Plasma Science*, vol. 47, no. 9, pp. 4350–4360, Sept. 2019, doi: 10.1109/TPS.2019.2934642

[13] J. Li, X. Zhong, J. Li, Z. Liang, W. Chen, Z. Li, and T. Li, "Theoretical analysis and experimental study on an avalanche transistor-based Marx generator," *IEEE Transactions on Plasma Science*, vol. 43, no. 10, pp. 3399–3405, Oct. 2015, doi: 10.1109/TPS.2015.2436373

[14] S. Vainshtein, J. Kostamovaara, V. Yuferev, W. Knap, A. Fatimy, and N. Diakonova, "Terahertz emission from collapsing field domains during switching of a gallium arsenide bipolar transistor," *Physical Review Letters*, vol. 99, no. 17, p. 176601, Oct. 2007, doi: 10.1103/PhysRevLett.99.176601